ELSEVIER

Physica A 235 (1997) 248–256

PHYSICA A

Microporous membrane filters: a static light scattering study

Luca Cipelletti, Marina Carpineti, Marzio Giglio *

Dipartimento di Fisica and INFM (Istituto Nazionale Fisica della Materia), Università di Milano, Via Celoria 16, 20133 Milano, Italy

Abstract

We studied some of the more employed microporous membrane filters via small-angle static light scattering under quasi-index matching conditions. We report data from both acetate of cellulose (AC) and mixed-esters of cellulose (MEC) membranes of various pore sizes p_s. On short length scales, the membranes have fractal morphology. While AC filters may be described as surface fractals, MEC membranes turn out to be mass fractals. Furthermore, the scattered intensity distributions exhibit a peak at a finite wave vector q_m, thus indicating the presence of a certain degree of spatial order over a characteristic length $\Lambda = 2\pi/q_m$. Λ is found to increase with p_s, as expected, although it is always larger than p_s and is not trivially related to it.

We propose a description of the membrane structure which accounts for the experimental results and is further corroborated by mass density measurements.

PACS: 61.43.Gt; 61.43.Hv

1. Introduction

Microporous membrane filters are employed in almost every laboratory. Their basic application is in particle and dust removal, but they are also used for other purposes, such as microbiological and sterility testing, gas analysis, electrophoresis and biological tissue simulation. Many materials and manufacturing techniques are used in the membrane production and this results in a wide variety of different membrane types [1, 2]. Filters are characterised by their sieving capability which is a measure of the smallest particle that cannot flow through the membrane without remaining trapped inside it. This value is supplied by the manufacturers and it is called *pore size* (p_s).

We focussed our attention to a particular class of membrane filters which are *sponge-like* on a microscopic scale. In particular, we used for the first time small-angle static

* Corresponding author.

PII S0378-4371(96)00345-7

light scattering for studying filters made of mixed-esters (acetate and nitrate) of cellulose (MEC) and of acetate of cellulose (AC), with pore sizes ranging from 0.1 μm to 8 μm. These filters are about 150 μm thick and, in air, they have a white mat appearance. In order to make light scattering measurements possible, we reduced the optical mismatch by immersing the membranes in a properly chosen solvent.

The experimental technique allows to obtain information about the inner microscopic structure of the membranes over length scales which are inversely proportional to the wave vector q ($q = 4\pi\lambda^{-1}\sin(\theta/2)$, where θ is the scattering angle and λ is the wavelength in the medium). We found that the intensity distributions $I(q)$ decay asymptotically according to a power law ($I(q) \propto q^{-\alpha}$) with non-integer exponent α. This is an evidence that over short length scales the membranes have an intrinsically disordered structure that may be described as fractal. In particular, we observed that α has different values for MEC and AC membranes, leading to the picture that AC membranes are porous solids with fractal pore surface (*surface fractals*), while MEC membranes may be described as *mass fractals*. By contrast, we observed that at smaller q values the intensity distributions exhibit a peak at wave vector $q_m \neq 0$ which indicates the existence of a certain degree of order over a typical length scale $\Lambda = 2\pi/q_m$. Λ was found to be always larger than the membrane's pore size p_s. Furthermore, different trends were found in the relation between Λ and p_s for the two membrane types. All these data, together with mass density measurements, suggest two different pictures for the morphology of MEC and AC membrane filters.

2. The experiment

We investigated Sartorius AC membrane filters with pore size ranging from 0.2 to 8 μm and Millipore MEC filters with p_s from 0.1 to 8 μm. Each measurement has been performed by filling a scattering cuvette with one membrane immersed in a solvent, chosen to reduce the optical contrast. As the refractive index of mixed esters of cellulose is $n \approx 1.51$ [1], and for acetate of cellulose $n \approx 1.47$ [2], we used different solvents for the two filter types. The choice of the solvent has been done for each sample in order to fully exploit the potentiality of small-angle light scattering. On one hand, we need to use samples which scatter at least a few percent of the incoming beam to reduce the noise in the measurements. In fact, collecting scattered light at very low angle has the disadvantage that spurious contributions due to stray light cannot be avoided and consequently, one needs a considerable amount of scattered light to obtain an acceptable signal to noise ratio. On the other hand, we want to work with small optical contrasts to avoid multiple scattering. In particular, membranes were immersed in an appropriate mixture of *p*-cymene (refractive index $n = 1.490$) and 1-bromonaphtalene ($n = 1.657$) with refractive indices chosen in the range $1.490 \leqslant n \leqslant 1.527$ in order to maintain the attenuation values between 2% and 20%.

While preparing the samples, the most serious problem turned out to be the presence of air inside the membranes. In fact, due to the very high refractive index mismatch,

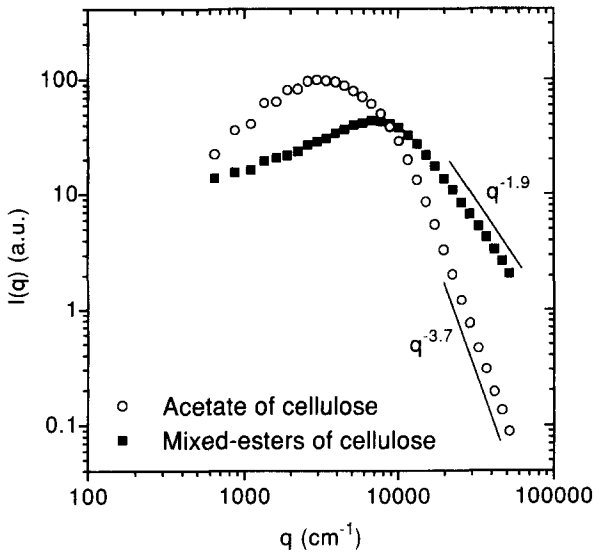

Fig. 1. Intensity distributions of the light scattered by two membrane filters with the same pore size (1.2 μm) but different chemical composition (open circles refer to the AC filter, squares to the MEC one).

air bubbles strongly scatter and at low angles their contribution can seriously disturb the measurements. In order to remove the air from the membranes, we placed them in the matching solvent and we outgassed the solution by means of a water jet pump. Ultrasound pulses were also used to improve the outgassing procedure. Finally, we did not purify the samples to remove dust particles. In fact, the filters are supplied by the manufacturers quite clean, as they have to be used exactly for removing dust. Conversely, any purifying procedure implies the handling of the sample and consequently, it can easily introduce extra dust.

The low angle light scattering setup allows to collect data at 31 angles simultaneously, thanks to a specially prepared sensor [3]. In the configuration used for this experiment, the range of accessible wave vectors q is either $3 \times 10^2\,\mathrm{cm}^{-1} \leqslant q \leqslant 3 \times 10^4\,\mathrm{cm}^{-1}$ or $6 \times 10^2\,\mathrm{cm}^{-1} \leqslant q \leqslant 5 \times 10^4\,\mathrm{cm}^{-1}$.

In Fig. 1 we show the intensity distributions of the light scattered by two filters with the same pore size, namely $p_s = 1.2\,\mu$m, but different chemical composition (AC and MEC), both immersed in pure p-Cymene. In spite of the presence of a peak at a finite wave vector q_m in both curves, their shapes look very different. As a first point, both curves decay asymptotically according to a power law $I(q) \propto q^{-\alpha}$, with $\alpha = 1.9$ for the MEC membrane and $\alpha = 3.7$ for the AC one. Although in Fig. 1 we only show the case of a particular pore size, we measured similar α values for all the MEC and AC filters whose asymptotic decay was in the range of accessible q vectors. The exponent α is very important for determining the morphology of the membranes. In fact, it is well known [4] that a power law asymptotic decay of the light scattered intensity distributions, with a non-integer exponent $\alpha < 4$, is typical of

fractals. In particular, two different fractal systems may be distinguished as a function of α. If $\alpha < 3$, the scattering object is a *mass fractal*, i.e. a self-similar object such that the minimum number N of cubes of edge l needed to cover it is given by:

$$N(l) \propto l^{-d_f} , \tag{1}$$

where d_f is the mass fractal dimension. In this case $\alpha = d_f$. By contrast, if $3 < \alpha < 4$, the scattering system is a solid object bounded by a fractal surface and is called *surface fractal*. Analogously to Eq. (1), the minimum number N of squares of side l needed to cover a fractal surface scales according to:

$$N(l) \propto l^{-d_s} , \tag{2}$$

where d_s is the surface fractal dimension. For these systems the exponent α is simply related to d_s, by relation $\alpha = 6 - d_s$.

The asymptotic behaviour of the intensity distributions shown in Fig. 1, therefore, indicates that on short length scale MEC membrane filters have a mass fractal morphology with $d_f = 1.9$, while for AC filters the fractality is confined to the boundary of the structure. Accordingly, AC membranes can be described as porous solids with fractal pore surfaces characterised by a surface fractal dimension $d_s = 6 - \alpha = 2.3$.

As we already pointed out, both the curves in Fig. 1 exhibit a pronounced peak at $q_m \neq 0$ and this is typical of structures with a certain degree of spatial order over a characteristic length $\Lambda = 2\pi/q_m$. It is probably not surprising that membrane filters, which are objects with a well-defined pore size, have a spatial periodicity over a certain length, and one could expect that the typical length Λ is simply related to p_s. By contrast, in Fig. 1 we observe that the peak position (and consequently Λ) is very different for MEC and AC membranes, although the two filters have the same pore size. Moreover, Λ is much larger than the pore size in both cases, being 8.4 μm for the MEC membrane and 22.4 μm for the AC one, to be compared to $p_s = 1.2$ μm. Therefore, the typical mass fluctuation length Λ does not seem to be simply related to the pore size, as it is much larger than p_s and it assumes different values for different membrane types. In order to determine the relation between Λ and p_s, we investigated how the scattered intensity distributions vary with the pore size for both types of membranes.

We show in Fig. 2 a set of intensity distributions scattered by AC membrane filters with $0.2\ \mu m \leqslant p_s \leqslant 8\ \mu m$, and in Fig. 3 the intensity scattered by MEC membranes with $0.1\ \mu m \leqslant p_s \leqslant 8\ \mu m$. It can be noticed that in both cases a peak at a finite wave vector is present for all values of p_s. The peak moves to higher q values as the pore size decreases, eventually falling outside the experimental range. This result clearly indicates that the typical mass density fluctuation length Λ grows with the pore size. The peak behaviour, however, is quite different for AC and MEC membranes, especially for the larger values of p_s. In fact, we notice that for MEC membranes (see Fig. 3) for $p_s \geqslant 3\ \mu m$ the peak position hardly changes, while this feature is not observed for AC filters (see Fig. 2). We can better appreciate this difference by comparing Figs. 4(a) to Fig. 5(a), where Λ versus p_s is shown for the AC and MEC membrane

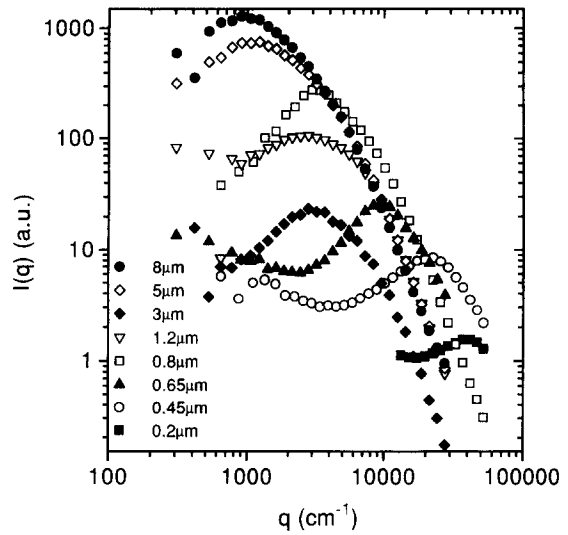

Fig. 2. Scattered light intensity for the AC membrane filters, with pore size ranging from 0.2 to 8 μm.

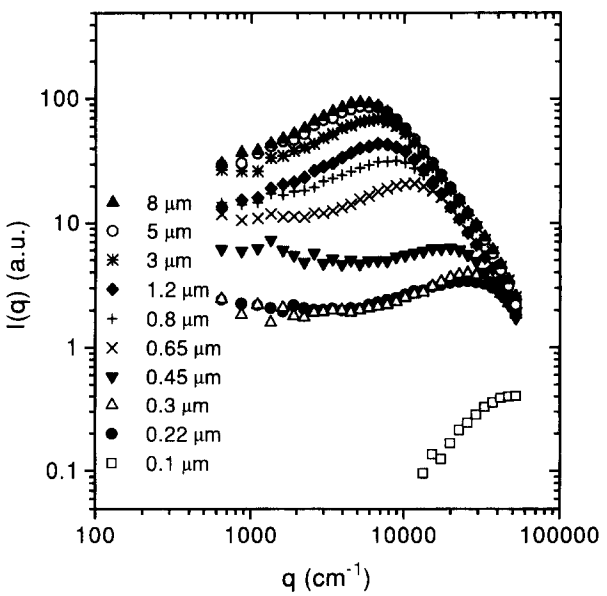

Fig. 3. Scattered light intensity for the MEC membrane filters, with pore size ranging from 0.1 to 8 μm.

filters, respectively. For AC membranes Λ varies roughly linearly with p_s in the whole range of pore sizes, while for MEC membranes two different growth trends may be distinguished. For smaller pore sizes ($p_s < 1.2\mu$m) there is a linear dependence between Λ and p_s, as in the case of AC membranes. This linear regime is evidenced in the

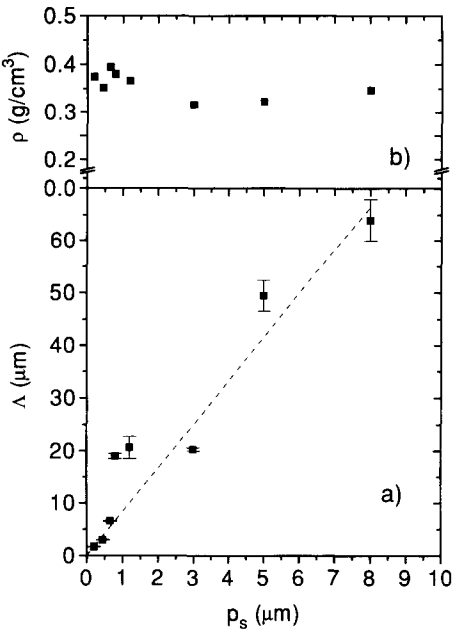

Fig. 4. Pore size dependence for the AC membrane filters of the mass density fluctuation length Λ (a) and the mass density ρ (b). The dashed line in (a) is a linear fit through the origin over the whole range of pore sizes.

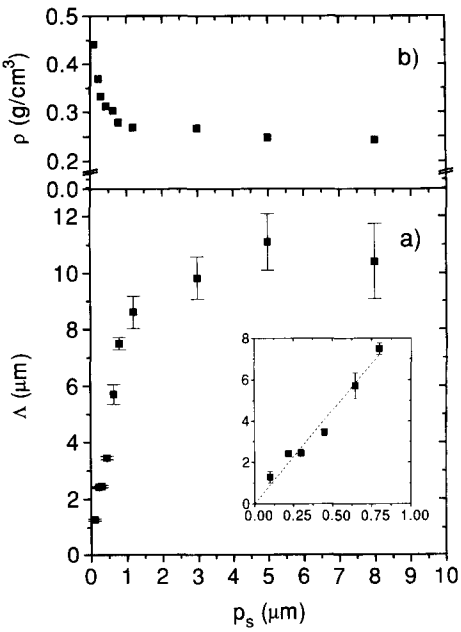

Fig. 5. Pore size dependence for the MEC membrane filters of the mass density fluctuation length Λ (a) and the mass density ρ (b). In the inset shown in (a), the dashed line is a linear fit through the origin for $p_s \leqslant 0.8$ μm.

inset of Fig. 5(a). It must be stressed that in the linear regime Λ is much larger than p_s and $\Lambda/p_s \cong 9$, similarly, to that observed for AC membranes, where $\Lambda/p_s \cong 7.8$. In contrast, for larger p_s, Λ only slightly increases and eventually tends to saturate reaching values comparable to those of the pore size.

The different dependence of Λ on p_s observed for the two filter types suggests that different pore sizes are obtained via structure modification which are not the same for the two kinds of membranes. In order to get more information on the structure differences between filters of various pore sizes and type, we also performed mass density measurements. Membrane mass density ρ as a function of the pore size p_s is shown in Figs. 4(b) and 5(b) for AC and MEC membranes, respectively. We observe a different trend in the two cases. For AC membranes ρ is almost constant over the whole range of pore sizes. On the contrary, for MEC membranes ρ decreases with the pore size for $p_s \leqslant 0.8\ \mu$m, while it is almost constant for larger p_s values.

3. Discussion and conclusions

To describe the membrane architecture it is important to understand the meaning of the typical length Λ and its relation to the pore size p_s. As a first point, we recall that the presence of a peak in the intensity distributions is typical of many physical systems as fluids undergoing spinodal decomposition processes [5], porous media [6–9], and more generally, of all those systems characterised by a mass anti-correlation over a characteristic length scale $\Lambda = 2\pi/q_m$ [10–12]. In other words, a peak shaped $I(q)$ indicates that each massive area is surrounded by a depletion region, where the probability of finding another massive zone is less than the average and Λ is the characteristic mass density fluctuation length. On the other hand, p_s is a measure of the largest particle which can flow through the membrane, and therefore, it is the smallest size of the connections between the filter voids that a particle is likely to pass through when moving across the membrane. Consequently, we expect the typical mass density fluctuation length Λ to be larger than p_s (as actually observed in Figs. 4(a) and 5(a)), due to the fact that Λ must be larger than the voids themselves. According to this explanation, Λ only constitutes an upper limit for p_s and its value depends on the inner morphology of the membrane. Therefore, it may happen that membranes with different Λ have the same pore size, as it is actually the case (see Fig. 1).

Let us now consider the different dependence of Λ on p_s observed for AC and MEC membrane filters. For this purpose mass density measurements turn out to be extremely clarifying, provided that the different fractal morphologies of AC and MEC membranes are properly taken into account. In particular, for AC membranes, Λ grows linearly with p_s and ρ is almost constant over the whole range of values of the pore size (see Fig. 4). In this case, light scattering data and mass density measurements both indicate that different sieving capabilities, i.e. different values of p_s, correspond to dilated or shrinked versions of the same structure, without appreciable changes in the filter morphology. In fact, we recall that AC membranes are surface fractals and,

as a consequence of the definition itself [13], mass density should not change if the structure is rescaled.

On the other hand, the data shown in Fig. 5 indicate that the rescaling model proposed for AC membranes may be applied only to MEC filters with pore size less than 1.2 μm. In fact, MEC filters are mass fractals and, at variance with surface fractals, mass density should decrease when dilating or shrinking the structure, without changing the morphology. This behaviour of ρ is actually observed for $p_s < 1.2$ μm, i.e. those values of the pore sizes for which Λ/p_s is constant. By contrast, for larger pore sizes both the scattering data and the mass density measurements suggest that the membrane structure does not appreciably change with the pore size. Our interpretation is that for p_s larger than 1.2 μm the sieving capability is changed without appreciably affecting the membrane architecture. We can intuitively describe this by imagining that some of the small and tenuous arms of the ramified structure which constitute the membrane are removed in order to obtain larger passages between the void areas and, therefore, larger pore sizes. In fact, while the presence of these arms can greatly affect the filter's sieving capability, they are only an insignificant amount of the overall membrane mass and, therefore, they can neither be detected by mass density measurements nor scatter enough light to appreciably affect the light scattering data.

In conclusion, we have shown that on short length scales microporous membrane filters do offer a wide spectrum of fractal morphologies being either surface or mass fractals. On larger length scales, they have a quasi-ordered structure characterised by a typical length Λ which is necessarily larger than the pore size p_s. Furthermore, the relation between Λ and p_s is not trivial and depends strongly on the filter type. Mass density measurements combined with light scattering data allow to depict the variation of filter architecture with pore size, depending on the different membrane types, thus explaining the observed dependence of Λ on p_s.

Acknowledgements

We are grateful to A. Riva and G. Rigamonti (Millipore S.p.A., Italy) for supplying some of the samples used in this work. This work has been supported by grants from the Ministero dell'Università e della Ricerca Scientifica e Tecnologica (MURST) and from the Consiglio Nazionale delle Ricerche (CNR).

References

[1] Millipore technical brochure, Millipore Corp., Ashby Road, Bedford, MA 01730.
[2] Sartorius technical brochure, Sartorius AG, P.O. Box 32 43, Weender Landstrasse 94-108, D-3400 Göttingen, Germany.
[3] M. Carpineti, F. Ferri, M. Giglio, E. Paganini and U. Perini, Phys. Rev. A 42 (1990) 7347.
[4] See, for example, S.K. Sinha, Physica D 38 (1989) 310; P. Pfeifer and M. Obert, in: The Fractal Approach to Hetrogeneous Chemistry, ed. D. Avnir (Wiley, Chichester, 1989).
[5] See for example J.D. Gunton, M. San Miguel and P.S. Sahni, in: Phase Transitions, Vol. 8 (Academic Press, London, 1983).

[6] P. Wiltzius, F.S. Bates, S.B. Dierker and G.D. Wignall, Phys. Rev. A 36 (1987) 2991.
[7] A. Höhr, H.-B. Neumann, P.W. Schmidt, P. Pfeifer and D. Avnir, Phys. Rev. B 38 (1988) 1462.
[8] P. Levitz, G. Ehret, S.K. Sinha and J.M. Drake, J. Chem. Phys. 95 (1991) 6151.
[9] P. Fratzl, G. Vogl and S. Klaumünzer, J. Appl. Crystallogr. 24 (1991) 588.
[10] K. Schätzel and B.J. Ackerson, Phys. Rev. Lett. 68 (1992) 337.
[11] M. Carpineti and M. Giglio, Phys. Rev. Lett. 68 (1992) 3327; J. Bibette, T.G. Mason, Hu Gang and D.A. Weitz, Phys. Rev. Lett. 69 (1992) 981.
[12] V. Degiorgio, G.P. Banfi, G. Righini and A. Rennie, Appl. Phys. Lett. 57 (1990) 2879.
[13] P.W. Shmidt, J. Appl. Crystallogr. 24 (1991) 414.